ACADEMIC PRESS

Biochemical and Biophysical Research Communications 293 (2002) 1550–1555

BBRC

www.academicpress.com

Visualization and force measurement of branching by Arp2/3 complex and N-WASP in actin filament

Ikuko Fujiwara,[a] Shiro Suetsugu,[b] Sotaro Uemura,[a] Tadaomi Takenawa,[b] and Shin'ichi Ishiwata[a,c,*]

[a] *Department of Physics, School of Science and Engineering, Waseda University, 3-4-1 Okubo, Shinjuku, Tokyo 169-8555, Japan*
[b] *Department of Biochemistry, Institute of Medical Science, University of Tokyo, Tokyo, Japan and CREST, Japan Science and Technology Corporation (JST), 4-6-1 Shirokanedai, Minato, Tokyo 108-8639, Japan*
[c] *Advanced Research Institute for Science and Engineering, Waseda University, 3-4-1 Okubo, Shinjuku, Tokyo 169-8555, Japan*

Received 22 April 2002

Abstract

To determine whether the Arp2/3 complex activated by N-WASP (VCA) branches actin filaments at the side (side branching), or at the barbed (B-)end (end branching) of the mother filaments, we have directly observed the branching process of actin filaments and examined single-molecule unbinding under optical microscope. We found that side branching was predominant, though not exclusive. At the initial stage of polymerization, the branching at the B-end occurred and subsequently the side branching started to occur. In either type of branching, the mother and daughter filaments elongated at nearly the same rate (growing type). Independently of the stage of polymerization, branching due to the direct coupling of filaments with an acute angle to the mother filaments (a coupling type) occurred. Phalloidin suppressed the growing type of branching but not the coupling type, implying that actin monomers are required for the former but not the latter. We found, by single molecule measurements using optical tweezers, that the Arp2/3 complex attaches to the side of actin filaments and the N-WASP appears to detach from the actin–Arp2/3 complex at 6–7 pN.

Keywords: Arp2/3 complex; VCA; N-WASP; Optical tweezers; Branching of actin filaments; Polymerization of actin; Total internal reflection fluorescence microscopy

Polymerization–depolymerization dynamics of actin filaments is a key process for many cellular events. The dynamics of the filaments is spatially and temporarily regulated by various kinds of functions of regulatory proteins such as capping, severing, and branching, together with control through the binding of Ca^{2+} and phosphorylation and so on. Among the regulatory proteins, the Arp2/3 complex and a WASP (Wiskott–Aldrich syndrome protein) family have recently been recognized as important for regulating polymerization of actin and creating fast-growing B-ends and for generating a branched actin filament network at the leading edge of moving cells [1–5].

All WASP family proteins have VCA (verprolin-homology, cofilin-homology, and acidic or C-terminal region of WASP family proteins) domain, a minimum region for the activation of Arp2/3 complex [6–9], which results in the formation of branched and mesh-like actin filaments [10]. Not only the electron microscopic structure [11] of Arp2/3 complex in the actin filament but also its crystal structure [12] have recently been determined, so that the mechanism of branching is going to be clarified on a molecular level. But, a controversy exists on the mechanism of branching of actin filaments, especially, on the branching from the side or the end of the mother actin filaments [13–16]. Although total internal reflection fluorescence microscopy [17] for imaging fluorescent single actin filaments has recently revealed a side branching that preferably occurs near the B-end [18–20], a more detailed analysis under different conditions is required to clarify the branching mechanism.

We examined how branching of actin filaments occurs during polymerization in the presence of Arp2/3

* Corresponding author. Fax: +81-3-5286-3437.
E-mail address: ishiwata@mn.waseda.ac.jp (S. Ishiwata).

0006-291X/02/$ - see front matter
PII: S0006-291X(02)00421-7

complex and VCA. As time proceeds after the addition of salts, not only the polymerization of individual actin filaments but also the branching of the filaments becomes observable. We could distinguish the branching from simple overlapping of two filaments by observing translational and bending Brownian movement of filaments.

Materials and methods

Preparation of proteins. Pure actin was prepared from rabbit muscle [21] except that tropomyosin–troponin complex was removed before preparing acetone powder according to Ebashi with slight modifications [22]. Bovine Arp2/3 complex was prepared according to a published protocol [23]. GST-fusion VCA was purified as described previously [7]. Fluorescent-dye labeling (100%) of Cys 374 of actin was done by tetramethylrhodamine-5-maleimide (TMR-5-MA, Molecular Probes) dissolved in dimethylformamide (a final concentration, less than 0.1%; Aldrich) in 0.1 M KCl, 1 mM $MgCl_2$, 0.2 mM ATP, and 10 mM imidazole buffer, pH 7.0. The free fluorescent-dye was removed by ultracentrifugation of the labeled F-actin solution and then by column chromatography (Sephadex G-25) of labeled G-actin solution.

Observation of polymerization and branching. Actin (42 kDa, 500 nM, of which 10 % was labeled with TMR-5-MA) in the presence of Arp2/3 complex (220 kDa, 70 nM) and GST-fusion VCA (39 kDa, 600 nM) was started to be polymerized in a test tube at time zero by addition of a polymerization buffer, i.e., 50 mM KCl, 1 mM $MgCl_2$, 4 mM ATP, 1 mM EGTA, 10 mM imidazole buffer, pH 7.0, 100 mM dithiothreitol, 20 μg/ml catalase, 100 μg/ml glucose oxidase, 3 mg/ml glucose, and 0.3 (w/v)% methylcellulose at room temperature (27 °C). Immediately after the addition of salt, the solution was put on a glass cover and the four sides of a cover slip were sealed with enamel, and then the microscopic observation was started. To image the filaments

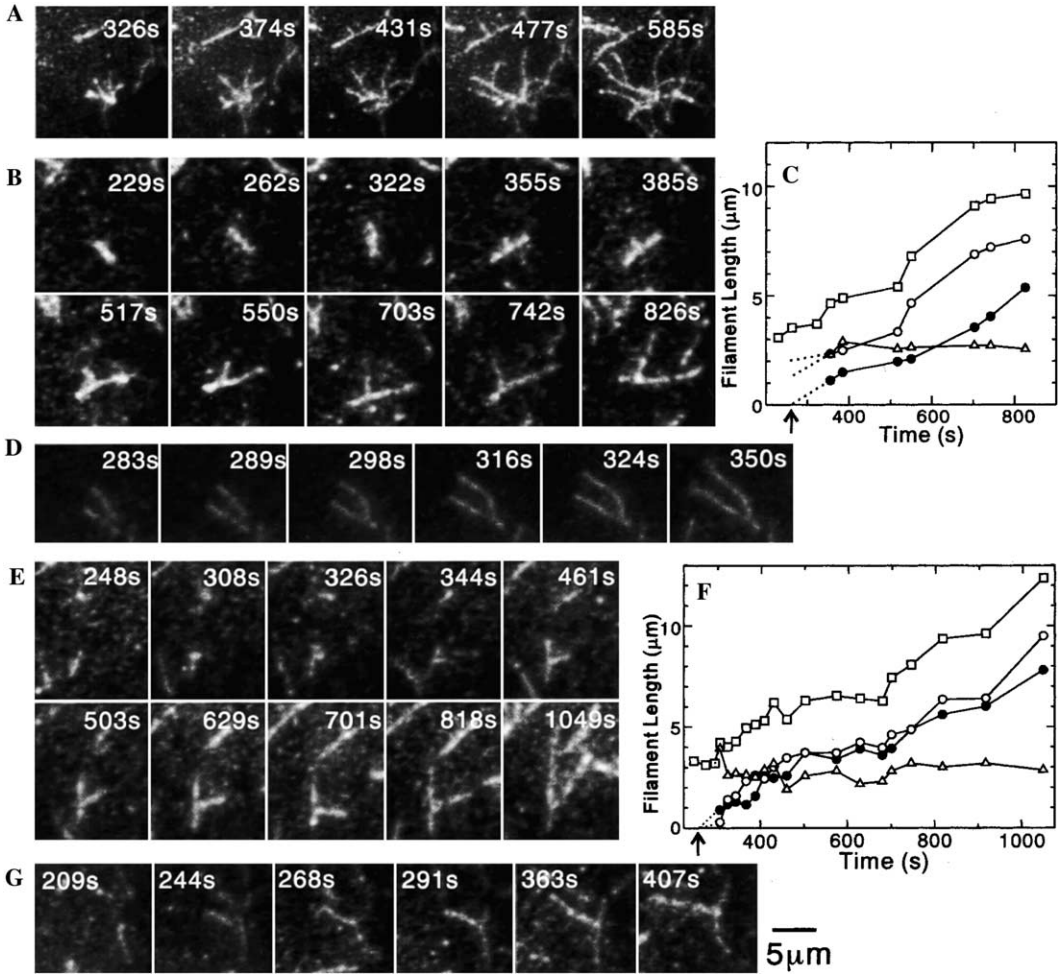

Fig. 1. Typical patterns of fluorescence image showing branching and polymerization of actin filaments observed in the presence of Arp2/3 complex and VCA and in the absence of phalloidin. (A) Formation of a dendritic network of actin filaments (movies are available at http://www.phys.waseda.ac.jp/bio/ishiwata/movies.html). (B) A growing type of side branching (movie). (C) Time course of the polymerization of the mother and daughter filaments in B. Here, open squares show total length, open circles the length between the B-end and the branching point, and open triangles the length between the P-end and the branching point of the mother filament. Closed circles show the length of the daughter filament. (D) A coupling type of side branching (movie). (E) A growing type of B-end branching (movie). (F) Time course of the polymerization of the mother and daughter filaments in E (symbols, the same as in C). (G) A coupling type of B-end branching (movie). The time (s) indicates that after the addition of salts. Scale bar, 5 μm.

in a high contrast, we added methylcellulose, which considerably suppressed the lateral Brownian movement of the filaments and partly the longitudinal movement. Note that the Brownian movement was too vigorous to obtain a clear fluorescence image of the filaments when the concentration of methylcellulose was less than 0.3%. When the effect of phalloidin was examined, the TMR-5-MA(10%)-labeled actin was first polymerized in the presence of phalloidin. The imaging of branching was begun just after the addition of the Arp2/3 complex and VCA to the actin filaments at room temperature (27 °C).

Microscopic analysis. Fluorescent dye-labeled single actin filaments were visualized by total internal reflection fluorescence microscopy (IX70, Olympus) with a green laser (#4301-050, μGreen) [17], which illuminates only ~150 nm in depth above the cover slip. Fluorescence images were collected using a SIT camera (C2400, Hamamatsu Photonics) equipped with an image intensifier (VS4-1815, Video Scope) and recorded on a Hi-8 video (EVO9650, Sony). To obtain the fluorescence image of high contrast for individual actin filaments, eight consecutive images taken at a video rate (for 0.27 s) were superimposed by using Scion image software (Scion Image). The spatial resolution was estimated to be 0.5 μm.

Microscopic measurement of unbinding force. To observe unbinding of an actin filament from the Arp2/3 complex with VCA by imposing external load, various concentrations (from 33 to 800 nM) of biotinylated VCA were attached to the cover slip. The cover slip was coated with avidin attached to the biotinylated BSA, which was adsorbed to the glass surface beforehand. The solution containing rhodamine phalloidin-labeled actin (6.6 nM) filaments and the Arp2/3 complex (12 nM), which was mixed just before the experiments, was infused into the cell. The bead (1 μm in diam)-tailed actin filaments (gelsolin, a B-end capping protein, was covalently fixed to the bead surface) were prepared according to the method previously described [24]. The bead was manipulated with optical tweezers of which trap stiffness was set to be 0.10 pN/nm. The loading rate used for measuring the unbinding force was 50.5 ± 17.3 pN/s (Ave. $\pm$ SD, $n = 61$). The position of the bead was determined from the centroid of a phase-contrast image of the bead using a frame memory computer (DIPS-C2000; Hamamatsu Photonics). The unbinding force (resolution, ± 0.2 pN) was estimated from the displacement of the bead from the trap center [25–27].

Results and discussion

Direct observation of several types of branching

The first example is a dendritic network grown from the nuclei composed of actin filaments (Fig. 1A). Among several types of branching, the most noticeable was growing of daughter filaments from the side of mother filaments (a growing type of side branching; Fig. 1B). In this example, the polymerization rates at the B-ends of the mother and daughter filaments were, respectively, 9.7×10^6 and 10.4×10^6 M/s, being nearly the same to each other; while that at the slow-growing pointed (P-)end of the mother filament was -0.28×10^6 M/s (Fig. 1C), both of which were consistent with the values obtained in solution [28]. Also, a direct coupling of daughter filaments with an acute angle to the side of the mother filament was observed (a coupling type of side branching; Fig. 1D). After the coupling occurred, the polymerization continued from both B-ends of the mother and daughter filaments at nearly the same rates.

Fig. 1E is an example attributed to a growing type of end branching (B-end branching unless otherwise stated; elongation of the two filaments from the same point, i.e., the B-end within the spatial resolution of optical microscope, was confirmed by rewinding the videotape). Both the mother and the daughter filaments polymerized at nearly the same rates, i.e., 9.0×10^6 and 7.5×10^6 M/s, respectively, whereas the polymerization rate at the P-end of the mother filament was -0.36×10^6 M/s (Fig. 1F). Thus, depolymerization occurred at the P-end of the mother filaments under the

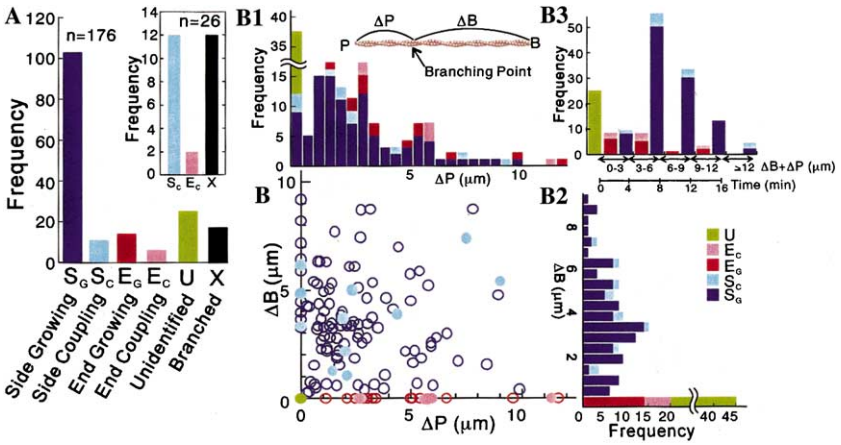

Fig. 2. Frequency of several types of branching. (A) Histogram showing the frequency of several types of branching in the presence of Arp2/3 complex and VCA and in the absence or the presence of phalloidin (inset). S_G, S_C, E_G, E_C, U, and X, respectively, growing type of side branching; coupling type of side branching; growing type of end branching; coupling type of end branching; *unidentified* (the type of branching could not be identified because the mother filaments were too short); and *already branched* at the beginning of observation. (B) Two-dimensional map showing the distribution of the distance of the branching point from the B-end (ΔB, ordinate) and the P-end (ΔP, abscissa) of mother filaments. (B1, B2, and B3) Frequency of several types of branching against ΔP (B1), ΔB (B2), and $\Delta B + \Delta P$ (total length of mother filaments; B3). The time on the abscissa of B3 was estimated from the average rate of polymerization (about 0.7 μm/min, Fig. 1C and F). The frequency of the B-end branching ($\Delta B = 0$) in B2 and that of the P-end branching ($\Delta P = 0$) in B1 are shown outside the abscissa and the ordinate of B, respectively.

given condition. Fig. 1G is an example showing direct coupling of the filament to the B-end of the mother filament. Also, we noticed that the frequency of head-to-tail annealing of filaments became about twice higher than that in the control, suggesting that the Arp2/3 complex activated by VCA increases the affinity of head-to-tail binding of filaments.

Analysis of branching mechanism

First, we classified the branching into several types. As summarized in Fig. 2A, excluding the data already branched at the beginning of the observation, about 72% was classified as side branching, 12% as end branching, and the remaining 16% as *unidentified* because the length of the mother filaments was too short.

Then, we examined how actin monomers are involved in these branching processes, so that the effect of phalloidin was examined. (On the polymerization process of pure actin in the presence of phalloidin, see [29].) As the inset of Fig. 2A shows, the growing type disappeared but the coupling type was still observed. Thus, we conclude that actin monomers are involved in the growing type of branching but not responsible for the direct coupling of daughter filaments.

Next, we quantitatively analyzed the data of the branching. The 2-D map in Fig. 2B shows the distance between either the B-end (ΔB on the ordinate) or the P-end (ΔP on the abscissa) of the mother filament and the branching point at the beginning of branching. From this 2-D map, we could extract the essential features of the branching, that is,

(1) at which part of the mother filaments the branching tends to occur. We made a projection of the frequency distribution to the ΔP and ΔB axes at every 0.5 μm interval (the limit of spatial resolution) as shown in Figs. 2B1 and B2, respectively. Fig. 2B1 shows that the frequency of side branching is higher at the P-end region of mother filaments. Moreover, note that the frequency of side branching is higher at the upper left portion of the line of $\Delta B = \Delta P$ in the 2-D map (Fig. 2B). This reflects a bias of side branching toward the P-end, which is in contrast to the previous observation that the side branching tended to occur at the B-end region [18]. We interpret this result as indicating that the binding of Arp2/3 complex to the side of actin filaments occurs as soon as the mother filaments began to polymerize, but the elongation of daughter filaments is delayed such that the polymerization of mother filaments proceeds. This apparent contradiction may be attributable to the difference in the experimental conditions between the two groups; the main difference is whether one is observing the polymerization process in solution without using nuclei in the presence of all the components (this study) or using pre-existing filaments fixed to the glass surface [18]. On the other hand, Fig. 2B2 shows that the frequency of branching at the B-end exceeds the average frequency of the side branching, suggesting that B-end branching occurs. The end branching may occur immediately after the binding of the Arp2/3 complex to the B-end of mother filaments. In this respect, it is interesting that the frequency of branching on short mother filaments (classified as *unidentified*) was high.

(2) The projection of the 2-D map along the total length of mother filaments ($=\Delta B + \Delta P$) (Fig. 2B3) shows what the most probable length of mother filaments for each type of branching is, in other words, *when* each type of branching occurs (note that the total length divided by the average polymerization rate represents the time after the beginning of polymerization). Fig. 2B3 shows that the B-end branching occurred at an early stage of polymerization and subsequently the side branching started to occur. Again, this is consistent with the above interpretation that the elongation of daughter filaments on the side branching is delayed.

Force measurement of branching

Next, we observed the binding of actin filaments to the Arp2/3 complex activated by VCA and measured its unbinding by imposing an external load (Fig. 3A). A fluorescence micrograph (Fig. 3B) shows how an actin filament was attached to and detached from the glass surface on which VCA and activated Arp2/3 complex are expected to be attached, demonstrating that the Arp2/3 complex and VCA certainly associate with the side of actin filaments. A possibility that the Arp2/3 complex is incorporated as a protomer into the mother filaments is excluded because the filaments were stabilized by phalloidin and gelsolin.

Fig. 3C shows the time course of the displacement of the bead from the trap center during the movement of the cover slip, so that each peak represents an unbinding event. Because VCA is firmly attached to the glass surface through the avidin–biotin bond, it is likely that detachment occurs at the interface between Arp2/3 complex and VCA. The fact that the filament once detached could reattach to the glass surface at the same point on the filament suggests that the Arp2/3 complex is remained attached to the side of actin filaments. We estimate that the unbinding force, of which distribution has a peak at 6–7 pN (Fig. 3D), is weaker than that for the actin-S1 rigor bonds [27], taking into account the high loading rate, 50 pN/s, used in the present study. From the relationship between the unbinding force and the binding lifetime [27] and the value of the unbinding force obtained here, we estimate that the binding lifetime in the absence of external load is shorter than 100 s, which is the one for the actin-S1 rigor bonds. On the other hand, the lifetime of the branch was longer than 10 min (data not shown), so that the lifetime of the binding of Arp2/3

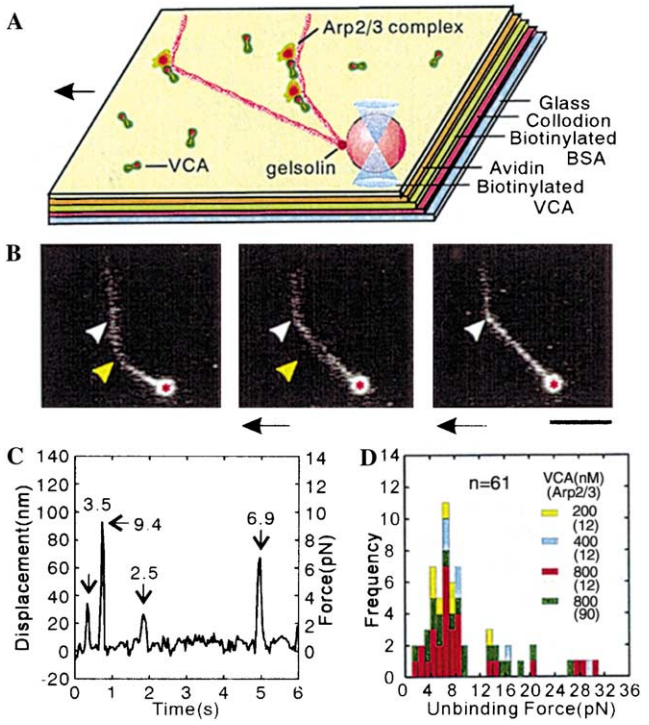

Fig. 3. Measurement of unbinding between a single actin filament and the Arp2/3 complex with VCA. (A) Schematic illustration showing how to measure the unbinding force by manipulating the bead, on which the B-end of an actin filament was attached, with optical tweezers. The external load was imposed by moving the cover slip toward the left at a constant rate (ca. 50 pN/s) as shown by a black arrow (also see arrows in B). (B) Fluorescence micrographs showing the unbinding of an actin filament from the VCA, which was attached to the glass surface through the biotin–avidin bond. Two arrowheads show the position where the VCA and the Arp2/3 complex must be located. The red asterisk shows the position of the trap center that was fixed. The VCA indicated by a yellow arrowhead was detached first, whereas the filament remained attached through the VCA indicated by a white arrowhead. The cover slip was manually moved toward the right when we tried the rebinding. After searching for the rebinding point, an external load was imposed again by moving the cover slip toward the left. Scale bar, 5 μm. (C) An example of raw data showing the time course of the displacement of the bead. The number at each peak indicates the unbinding force, which was obtained by multiplying the displacement of the bead and the trap stiffness (0.10 pN/nm) together. (D) Histogram showing the unbinding force distribution under various combinations of the concentrations of VCA and Arp2/3 complex. We found that the attachment of actin filaments to the glass surface was observed only at the VCA concentrations higher than about 200 nM. As the VCA concentration was increased, the linear density of the attachment points along the actin filament increased. We confirmed that the biotinylated BSA did not detach from the collodion-coated glass surface under the conditions examined here.

complex and an actin filament is expected to be an order of magnitude longer than that characteristic of the binding examined here.

A model of branching

Finally, we propose a model of branching mechanism based on the above analysis. As illustrated in Fig. 4,

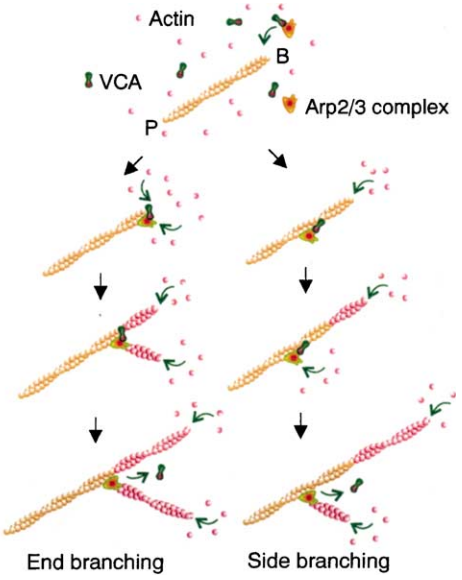

Fig. 4. Schematic illustration showing the two types of branching mechanism. The end branching (left column) and the side branching (right column), due to the binding of the Arp2/3 complex and VCA, respectively, to the B-end and to the side of the actin filament, are illustrated as proposed according to the present results.

accompanying the polymerization of actin, the Arp2/3 complex activated by VCA attaches to the actin filaments, so that the branching at the B-end of the mother filaments occurs at the same time and at the same polymerization rate on the mother and daughter filaments. The Arp2/3 complex also attaches to the side of the actin filaments (as evidenced by the unbinding force measurements), so that the daughter filament starts to polymerize but a little *behind* the B-end branching (Fig. 2B3). Even in the side branching, once the polymerization starts, the rate becomes the same (Fig. 1C). Note that, as far as the frequency is concerned, the side branching is definitely major, probably because the number of Arp2/3 complex attached to the side of actin filaments is much larger than that at the B-end. In addition to the growing type of branching, the coupling type of branching occurs regardless of the timing (Fig. 2B3). Hence, at least under the present experimental conditions, both the end branching and the side branching of growing type and coupling type occur with different timings and different frequencies. The temporal and spatial regulation of such differing types of branching takes place in various situations in vivo via several kinds of regulatory proteins in addition to the Arp2/3 complex and the WASP family proteins. The regulatory mechanism of branching will be clarified in greater detail by applying the technique of single filament imaging and manipulation as presented here to various combinations of regulatory proteins under various conditions.

Acknowledgments

We thank Drs. H. Tadakuma and T. Funatsu of Waseda University for technical assistance and discussion, and Dr. W. Rozycki of Waseda University for reading the manuscript. This research was partly supported by Grants-in-Aid for Scientific Research, for Scientific Research on Priority Areas, and for Bio-venture Project from the Ministry of Education, Culture, Sports, Science, and Technology of Japan, and by Grants-in-Aid from the Japan Science and Technology Corporation (CREST) and the Mitsubishi Foundation. We also thank colleagues at Waseda University and CREST for their encouragement and support.

References

[1] T.D. Pollard, L. Blanchoin, R.D. Mullins, Molecular mechanisms controlling actin filament dynamics in nonmuscle cells, Annu. Rev. Biophys. Biomol. Struct. 29 (2000) 545–576.
[2] D. Pantaloni, C. Le-Clainche, M.-F. Carlier, Mechanism of actin-based motility, Science 292 (2001) 1502–1506.
[3] J. Condeelis, How is actin polymerization nucleated in vivo? Trends Cell Biol. 11 (2001) 288–293.
[4] T. Takenawa, H. Miki, WASP and WAVE family proteins: key molecules for rapid rearrangement of cortical actin filaments and cell movement, J. Cell Sci. 114 (2001) 1801–1809.
[5] T.M. Svitkina, G.G. Borisy, Arp2/3 complex and actin depolymerizing factor/cofilin in dendritic organization and treadmilling of actin filament array in lamellipodia, J. Cell Biol. 145 (1999) 1009–1026.
[6] L.M. Machesky, R.D. Mullins, H.N. Higgs, D.A. Kaiser, L. Blanchoin, R.C. May, M.E. Hall, T.D. Pollard, Scar, a WASP-related protein, activates nucleation of actin filaments by the Arp2/3 complex, Proc. Natl. Acad. Sci. USA 96 (1999) 3739–3744.
[7] H. Miki, K. Miura, T. Takenawa, N-WASP, a novel actin-depolymerizing protein, regulates the cortical cytoskeletal rearrangement in a PIP2-dependent manner downstream of tyrosine kinases, EMBO J. 15 (1996) 5326–5335.
[8] H. Miki, T. Sasaki, Y. Takai, T. Takenawa, Induction of filopodium formation by WASP-related actin-depolymerizing protein N-WASP, Nature 391 (1998) 93–96.
[9] S. Suetsugu, H. Miki, H. Yamaguchi, T. Obinata, T. Takenawa, Enhancement of branching efficiency by the actin filament-binding activity of N-WASP/WAVE2, J. Cell Sci. 114 (2001) 4533–4542.
[10] H. Miki, T. Takenawa, Direct binding of the verprolin-homology domain in N-WASP to actin is essential for cytoskeletal reorganization, Biochem. Biophys. Res. Commun. 243 (1998) 73–78.
[11] N. Volkmann, K.J. Amann, S. Stoilova-McPhie, C. Egile, D.C. Winter, L. Hazelwood, J.E. Heuser, R. Li, T.D. Pollard, D. Hanein, Structure of Arp2/3 complex in its activated state and in actin filament branch junctions, Science 293 (2001) 2456–2459.
[12] R.C. Robinson, K. Turbedsky, D.A. Kaiser, J.B. Marchand, H.N. Higgs, S. Choe, T.D. Pollard, Crystal structure of Arp2/3 complex, Science 294 (2001) 1679–1684.
[13] K.J. Amann, T.D. Pollard, The Arp2/3 complex nucleates actin filament branches from the sides of pre-existing filaments, Nat. Cell Biol. 3 (2001) 306–310.
[14] L. Blanchoin, K.J. Amann, H.N. Higgs, J.B. Marchand, D.A. Kaiser, T.D. Pollard, Direct observation of dendritic actin filament networks nucleated by Arp2/3 complex and WASP/Scar proteins, Nature 404 (2000) 1007–1011.
[15] D. Pantaloni, R. Boujemaa, D. Didry, P. Gounon, M.-F. Carlier, The Arp2/3 complex branches filament barbed ends: functional antagonism with capping proteins, Nat. Cell Biol. 2 (2000) 385–391.
[16] R. Boujemaa-Paterski, E. Gouin, G. Hansen, S. Samarin, C. Le-Clainche, D. Didry, P. Dehoux, P. Cossart, C. Kocks, M.F. Carlier, D. Pantaloni, Listeria protein ActA mimics WASP family proteins: it activates filament barbed end branching by Arp2/3 complex, Biochemistry 40 (2001) 11390–11404.
[17] T. Funatsu, Y. Harada, M. Tokunaga, K. Saito, T. Yanagida, Imaging of single fluorescent molecules and individual ATP turnovers by single myosin molecules in aqueous solution, Nature 374 (1995) 555–559.
[18] J.K. Amann, T.D. Pollard, Direct real-time observation of actin filament branching mediated by Arp2/3 complex using total internal reflection fluorescence microscopy, Proc. Natl. Acad. Sci. USA 98 (2001) 15009–15013.
[19] J.A. Cooper, M.A. Wear, A.M. Weaver, Arp2/3 complex: advances on the inner workings of a molecular machine, Cell 107 (2001) 703–705.
[20] I. Ichetovkin, W. Grant, J. Condeelis, Cofilin produces newly polymerized actin filaments that are preferred for dendritic nucleation by the Arp2/3 complex, Curr. Biol. 12 (2002) 79–84.
[21] J.A. Spudich, S. Watt, The regulation of rabbit skeletal muscle contraction. I. Biochemical studies of the interaction of the tropomyosin–troponin complex with actin and the proteolytic fragments of myosin, J. Biol. Chem. 246 (1971) 4866–4871.
[22] H. Kondo, S. Ishiwata, Uni-directional growth of F-actin, J. Biochem. 79 (1976) 159–171.
[23] H. Yamaguchi, H. Miki, S. Suetsugu, L. Ma, M.W. Kirschner, T. Takenawa, Two tandem verprolin homology domains are necessary for a strong activation of Arp2/3 complex-induced actin polymerization and induction of microspike formation by N-WASP, Proc. Natl. Acad. Sci. USA 97 (2000) 12631–12636.
[24] N. Suzuki, H. Miyata, S. Ishiwata, K. Kinosita Jr., Preparation of bead-tailed actin filaments: estimation of the torque produced by the sliding force in an in vitro motility assay, Biophys. J. 70 (1996) 401–408.
[25] H. Miyata, H. Yoshikawa, H. Hakozaki, N. Suzuki, T. Furuno, A. Ikegami, K. Kinosita Jr., T. Nishizaka, S. Ishiwata, Mechanical measurements of single actomyosin motor force, Biophys. J. 68 (1995) 286s–290s.
[26] T. Nishizaka, H. Miyata, H. Yoshikawa, S. Ishiwata, K. Kinosita Jr., Unbinding force of a single motor molecule of muscle measured using optical tweezers, Nature 377 (1995) 251–254.
[27] T. Nishizaka, R. Seo, H. Tadakuma, K. Kinosita Jr., S. Ishiwata, Characterization of single actomyosin rigor bonds: load dependence of lifetime and mechanical properties, Biophys. J. 79 (2000) 962–974.
[28] T.D. Pollard, J.A. Cooper, Actin and actin-binding proteins. A critical evaluation of mechanisms and functions., Annu. Rev. Biochem. 55 (1986) 987–1035.
[29] S. Ishiwata, J. Tadashige, I. Masui, T. Nishizaka, K. Kinosita Jr., Microscopic analysis of polymerization and fragmentation of individual actin filaments, in: C.G. dos Remedios, D.D. Thomas (Eds.), Molecular Interactions of Actin, Springer, Heidelberg, 2001, pp. 79–94.